Cancer Letters 414 (2018) 190–204

Contents lists available at ScienceDirect

Cancer Letters

journal homepage: www.elsevier.com/locate/canlet

Original Article

ETS1 induction by the microenvironment promotes ovarian cancer metastasis through focal adhesion kinase

Sunil Tomar [a, 1], Joshua P. Plotnik [a, 1], James Haley [a, 1], Joshua Scantland [a], Subramanyam Dasari [a], Zahir Sheikh [a], Robert Emerson [b], Dean Lenz [c], Peter C. Hollenhorst [a, d, e], Anirban K. Mitra [a, d, f, *]

[a] Medical Sciences Program, Indiana University School of Medicine, Bloomington, IN, United States
[b] Department of Pathology and Laboratory Medicine, Indiana University, Indianapolis, IN, United States
[c] Urology, IU Health Southern Indiana Physicians, Bloomington, IN, United States
[d] Indiana University Melvin and Bren Simon Cancer Center, Indianapolis, IN, United States
[e] Department of Biochemistry and Molecular Biology, Indiana University School of Medicine, Indianapolis, IN, United States
[f] Department of Medical and Molecular Genetics, Indiana University School of Medicine, Indianapolis, IN, United States

ARTICLE INFO

Article history:
Received 18 August 2017
Received in revised form
23 October 2017
Accepted 11 November 2017

Keywords:
Ovarian cancer
Metastasis
Microenvironment
ETS1
FAK
Omentum

ABSTRACT

Metastatic colonization involves paracrine/juxtacrine interactions with the microenvironment inducing an adaptive response through transcriptional regulation. However, the identities of transcription factors (TFs) induced by the metastatic microenvironment in ovarian cancer (OC) and their mechanism of action is poorly understood. Using an organotypic 3D culture model recapitulating the early events of metastasis, we identified ETS1 as the most upregulated member of the ETS family of TFs in metastasizing OC cells as they interacted with the microenvironment. ETS1 was regulated by p44/42 MAP kinase signaling activated in the OC cells interacting with mesothelial cells at the metastatic site. Human OC tumors had increased expression of ETS1, which predicted poor prognosis. ETS1 regulated OC metastasis both *in vitro* and in mouse xenografts. A combination of ChIP-seq and RNA-seq analysis and functional rescue experiments revealed FAK as the key transcriptional target and downstream effector of ETS1. Taken together, our results indicate that ETS1 is an essential transcription factor induced in OC cells by the microenvironment, which promotes metastatic colonization though the transcriptional upregulation of its target FAK.

1. Introduction

Ovarian cancer (OC) is the deadliest gynecologic malignancy and fifth leading cause for cancer related deaths among women in USA [1]. At the time of diagnosis, the disease has already spread beyond the primary tumor in most patients and this is the main cause of OC related complications and morbidity [2,3]. However, our understanding of the regulation of the different steps of metastasis remains limited [4]. OC cells typically metastasize to mesothelium-covered peritoneal organs, and favorable interactions with the mesothelial cells and the underlying basement membrane are essential for successful colonization of the omentum, peritoneum, intestine, liver and other sites [5,6]. While it is widely accepted that colonization of the distant metastatic site is the rate-limiting step of metastasis [7,8], not much is known about the underlying mechanisms that regulate this process. This knowledge is limited due to the lack of appropriate experimental models to specifically investigate this key step. However, of late, some groups have devised *in vitro* 3D culture models to mimic the early steps of colonization [9]. Such models have yielded new insights into the process of colonization.

Abbreviations: OC, ovarian cancer; TF, Transcription factor; FAK, Focal adhesion kinase; MAP kinase, Mitogen activated protein kinase; HPMC, Human primary mesothelial cells.

* Corresponding author. 915 E. 3rd Street, Myers Hall 200C, Bloomington, IN 47405, United States.
E-mail address: anmitra@indiana.edu (A.K. Mitra).

[1] Authors have contributed equally.

https://doi.org/10.1016/j.canlet.2017.11.012

Paracrine/juxtacrine interactions with the microenvironment of the metastatic site are critical for metastasis. The microenvironment of the metastasis site can influence the gene expression patterns of the cancer cells determining their ability to establish metastatic colonies [8]. Therefore, the initial interaction of OC cells with mesothelial cells, the underlying basement membrane and fibroblasts plays a crucial role in successful metastasis [10]. A greater understanding of the underlying mechanism of regulation of gene expression through signals from the microenvironment is essential to target metastasis. Transcription factors (TFs) play a major role in regulation of gene expression and several important TF families have been implicated in OC [11–14]. In particular, the ETS family of TFs has been shown to promote cellular migration and invasion through the activation of genes such as matrix metalloproteases [15,16]. ETS1 regulates a wide variety of pro-tumorigenic effects [17] and is reported as a marker of poor survival in OC and is associated with the clinical stage and grade of the tumor [18,19]. However, the identity of the ETS factors that mediate OC metastatic colonization, and the role of the tumor microenvironment in this function are unclear.

Using an *in vitro* organotypic 3D culture model of the omentum [20] which physiologically replicates the early steps of metastatic colonization of OC, we have studied the potential deregulation of oncogenic ETS transcription factors in OC cells as a result of the cross-talk with the microenvironment. We report the upregulation of ETS1 as a key event, which enhances the OC cells' ability to metastasize both *in vitro* and *in vivo*. Moreover, by genomic profiling of ETS1 binding sites, transcriptomic and functional analyses, ETS1 was found to manifest its effects through the transcriptional upregulation of focal adhesion kinase (FAK).

2. Materials and methods

2.1. Reagents

Trypsin, Dulbecco's Modified Eagle Medium (DMEM), MEM vitamins, MEM nonessential amino acids and Penicillin-Streptomycin were purchased from Media Tech (Manassas, VA). TaqMan gene expression assay for ETS1 was obtained from Applied Biosystems (Foster City, CA). Silencer™ Select ETS1 siRNA, FAK siRNA and scrambled negative control were from Ambion (Austin, TX). Giemsa stain (Catalog # GS500) and crystal violet (Catalog #C0775) were obtained from Sigma Aldrich. Thiazolyl blue tetrazolium bromide was from Acros Organics (Catalog # 298-93-1) and 4% paraformaldehyde solution was purchased from Fisher Scientific (NC9245948).

2.2. Cell lines

The OC cell lines HeyA8, OVCAR5 and OVCAR8 were obtained from Ernst Lengyel, University of Chicago. Kuramochi cells were obtained from Japanese Collection of Research Bioresources and OVCAR4 from Joanna Burdette, University of Illinois at Chicago. All cell lines were grown in DMEM with 10% FBS along with 1% MEM vitamins, MEM nonessential amino acids and Penicillin-Streptomycin. Idexx BioResearch's (Columbia, MO) validation services for genetic validation of cell lines using CellCheck 16 (16 Marker STR Profile and Inter-species Contamination Test) and mycoplasma testing (Stat-Myco) was used to test all cell lines.

2.3. Isolation and culture of primary cells and assembly of the 3D culture

Omentum was obtained from female patients undergoing surgery for benign conditions in the Indiana University Heath Bloomington Hospital were used to isolate primary human mesothelial cells (HPMC) and normal omental fibroblasts (NOF) as described previously [20]. The primary cells were cultured in DMEM with 10% FBS and were used to assemble the 3D omental cultures as described previously [20]. Briefly, 360,000 NOFs with 91 μg of Collagen Type I (Rat tail, BD Cat#354236) were first seeded in 10 cm dishes and 3.6×10^6 HPMCs were seeded on top following attachment, to form a confluent monolayer. The 3D culture was allowed to grow for 24 h to enable secretion of growth factors and ECMs by the cells and subsequently used for experiments to investigate the initial events of colonization. OC cells (1×10^6) expressing GFP or labeled with cell tracker green (Molecular Probes Cat# C2925) were seeded on the 3D culture and allowed to grow for 2 days. The cancer cells were isolated by fluorescence activated cell sorting (FACS) and used for RNA/protein isolation. To set up the 3D culture in transwell inserts or 6 well plates, the number of cells and the amount of collagen were proportionately reduced according to the growth surface area. The Institutional Regulatory Board of Indiana University approved this research and informed consent was obtained from all patients.

2.4. Real-time PCR

RNA was isolated from the cells using miRNeasy Kit (Qiagen Catalog # 217004) and 0.5 μg RNA was used for reverse transcription using Applied Biosystems High Capacity Reverse Transcription Kit (Catalog # 4368813) on a Veriti 96-well thermal cycler (Applied Biosystems). Quantitative real-time PCR (qPCR) for ETS1, BCL2L12, SFN, ZNF114, EHD1, PTK2, CDH1, ZEB2 and FN1 expression was performed using TaqMan gene expression assay kit according to the manufacturer's protocol using Roche LightCycler 96 system. GAPDH was used as an endogenous control. ETS family member real-time qPCR was carried out as described previously [21]. The list of primers used is provided in Supplementary Fig. 1.

2.5. OC tissue microarray (TMA)

An OC TMA assembled in the Indiana University Simon Cancer Center consisting of formalin fixed paraffin embedded cores from 23 ovarian tumors and 6 normal fallopian tubes was stained for ETS1 with anti-ETS1 antibody (Aviva Systems Biology Catalog #: P100604_T100) by the Indiana University School of Medicine's Pathology and Laboratory Medicine core facility. The ETS1 nuclear expression was scored by a pathologist using a scale of 0 none, 1 weak, 2 moderate and 3 strong.

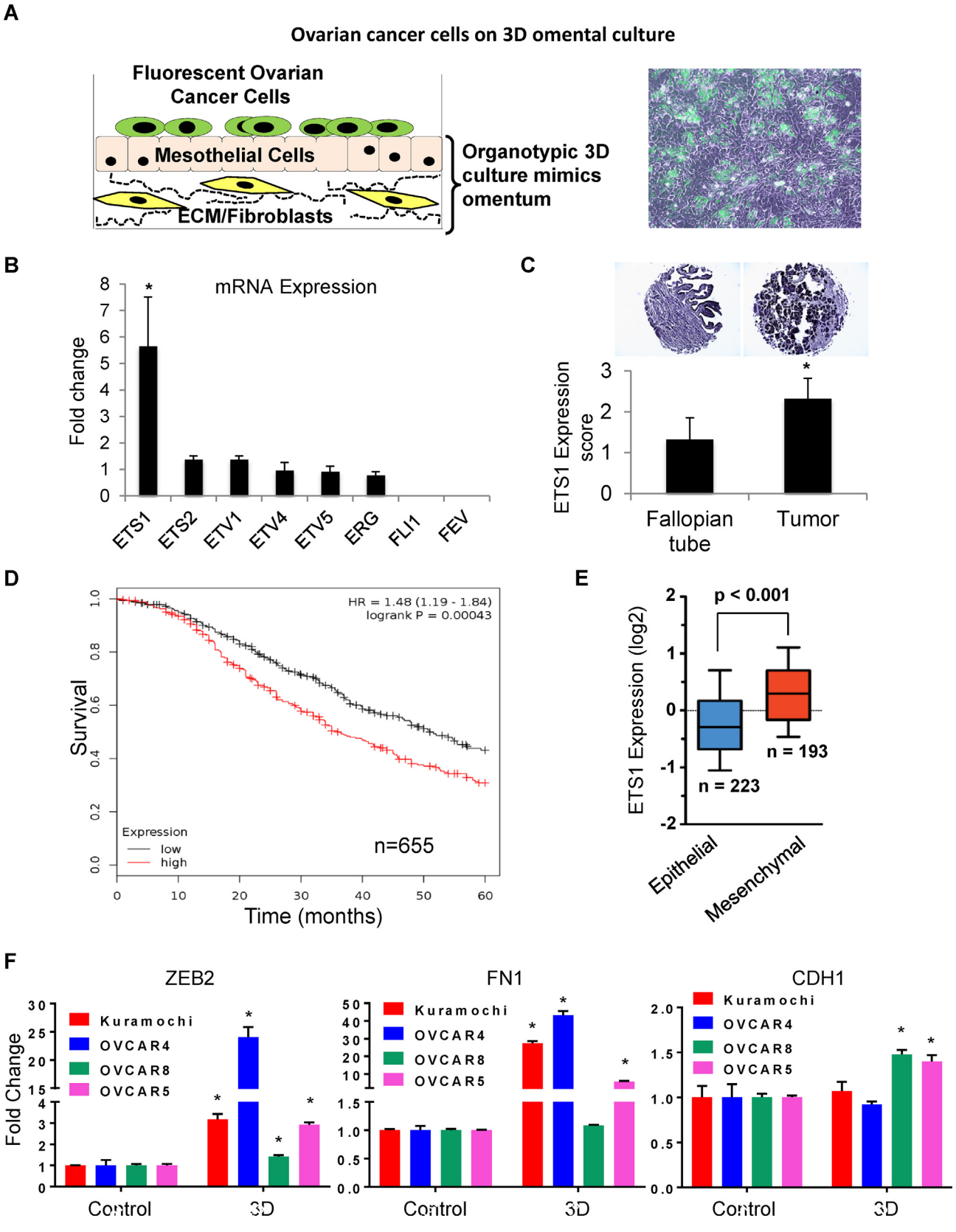
A
Ovarian cancer cells on 3D omental culture
Fluorescent Ovarian Cancer Cells
Mesothelial Cells
ECM/Fibroblasts
Organotypic 3D culture mimics omentum
B
mRNA Expression
Fold change
ETS1
ETS2
ETV1
ETV4
ETV5
ERG
FLI1
FEV
C
ETS1 Expression score
Fallopian tube
Tumor
D
HR = 1.48 (1.19 - 1.84)
logrank P = 0.00043
Survival
Expression
low
high
n=655
Time (months)
E
p < 0.001
ETS1 Expression (log2)
n = 193
n = 223
Epithelial
Mesenchymal
F
ZEB2
FN1
CDH1
Kuramochi
OVCAR4
OVCAR8
OVCAR5
Fold Change
Control
3D

2.6. Transient transfection

OC cells were transiently transfected with 30 nM ETS1, PTK2 or scrambled control siRNA using TransIT-X2 (Mirus Bio Cat# MIR 6000) following the manufacturer's protocol. For plasmid transfections, 2–3 μg plasmid was transfected using FuGENE HD (Promega Cat# E2311) or TransIT-2020 (Mirus Bio Cat# MIR 5400) as per the manufacturer's protocol. The cells were used for experiments 48 h after transfection or as indicated.

2.7. Migration

Transwell migration assays were conducted using 8 μm pore size inserts (BD, Falcon) as described previously [22]. OC cells were seeded in the upper chamber in 500 μl DMEM and allowed to migrate for 3–6 h at 37 °C. DMEM with 10% FBS was used as a chemoattractant in the lower chamber. Cells were fixed in 4% paraformaldehyde and imaged (5 fields/insert) using an EVOS FL Auto microscope (Life Technologies).

2.8. Proliferation

Proliferation assay was performed as described previously [22]. Briefly, OC cells were seeded in 96-well plates in 8 replicates (2000 cells/well) and allowed to grow for 5 days. On the fifth day MTT (3-(4,5-dimethylthiazol-2-yl)-2,5-diphenyltetrazolium bromide) Assay was conducted to measure proliferation of the OC cells. The absorbance was measured at 560 nm and adjusted for background absorbance at 670 nm using a SynergyH1 plate reader (BioTek).

2.9. Colony formation

Colony formation assay was performed as described previously [22]. Briefly, OC cells were seeded in 6 well plates (1000 cells/well) and allowed to form colonies. Once visible colonies were formed, they were fixed with 4% paraformaldehyde and stained with 0.005% crystal violet and were imaged using a Syngene G:Box imaging system and the number of colonies/well were counted.

2.10. Invasion through 3D culture

Cellular invasion through the surface of the omentum was assayed *in vitro* by first assembling the 3D culture on 8 μm pore size Fluoroblock transwell inserts in 24 well plates. GFP-expressing OvCa cells were then seeded on the 3D culture in the transwell insert in 200 μl serum-free DMEM. DMEM with 10% FBS served as a chemoattractant in the lower chamber. Cells were allowed to invade for 16 h and then were fixed with 4% paraformaldehyde. The fluorescent cancer cells that had invaded were imaged (5 fields/insert) using an EVOS FL Auto microscope (Life Technologies).

2.11. Colony formation on 3D culture

3D culture was set up in 6 well plates as described above and OC cells expressing GFP were seeded in the plates (1000 cells/well) and allowed to form colonies on the 3D culture. The green fluorescent colonies were imaged using a Syngene G:Box imaging system and the number of colonies/well were counted.

2.12. Generation of CRISPR/Cas9 ETS1 knockout cell lines

ETS1 KO cell lines were generated using LentiCRISPRv2 plasmid (Zhang, Addgene # 52961). Guide RNA's (gRNA) were generated using algorithms found at crispr.mit.edu and can be found in Supplementary Fig. 1 gRNA's were annealed and cloned into the Cas9 backbone [23] and lentiviral particles were produced. After production, cells were transduced with virus and selected with puromycin (5 μg/mL) was added at 24hr. Stably transfected cells were counted and diluted to a concentration of 1 cell/200μL. In a 96-well plate, 100 μL of diluted cells were plated and allowed to grow to confluence. Wells containing cells were expanded into 24-well, then into 6-well tissue culture plates. Once near confluency, single colonies were tested for knockout efficiency via protein immunoblotting. Identification of CRISPR/Cas9 generated indels were accomplished via gDNA PCR and sequencing individual clones ligated into pet19 (NEB) (Supplementary Fig. 2).

2.13. Mouse xenograft model of OvCa metastasis

The mouse xenograft model of OC metastasis was used as described previously [10]. Briefly, 6 weeks old, female, athymic nude mice were randomized into two groups (9 mice/group) and were injected intraperitoneally (i.p.) with 1×10^6 HeyA8 cells either wild type or with ETS1 knock out. Mice were euthanized 15 days post-injection and the tumors were surgically resected and weighed.

2.14. Chromatin immunoprecipitation and sequencing

ChIP was carried out as previously described [24]. In short, cells were cross-linked using 1% v/v Formaldehyde (Fisher Scientific) for 15 min and quenched with 2 M Glycine for 5 min. Isolated cells were lysed and sonicated for 3 min (30 s ON/OFF) [Daigenode, Bioruptor Pico]. Nuclear lysate was rotated with

Fig. 1. ETS1 is upregulated in OC. (**A**) *Left:* The orthotopic *in vitro* omental 3D culture model, which replicates the outer layers of the omentum. The GFP expressing OC cells were seeded on the 3D culture and allowed to grow for 2 days. The OC cells were then isolated using FACS and their RNA was isolated to estimate the expression levels of oncogenic ETS factors by qPCR. *Right:* An image of GFP expressing OC cells growing on the 3D culture. (**B**) qPCR was done to determine the expression of ETS factors in OVCAR8 cells seeded on 3D culture and data is expressed as fold change compared to control cells seeded on normal cell culture dishes. FLI1 and FEV had no expression in these cells. The error bars represent standard deviations from 3 independent experiments. *$p < 0.01$, Students *t*-test (**C**) An OC TMA consisting of 23 OC tumors and 6 normal fallopian tubes was stained for ETS1 and a pathologist scored the nuclear ETS1 expression. The ETS1 expression in the OC tumors and normal fallopian tubes are plotted and representative images of the tissue cores are shown above. *$p < 0.01$, Students *t*-test. (**D**) Kaplan-Meier plot depicting the 5-year survival of ovarian cancer patients with high (red) or low (black) expression of ETS1 was analyzed using KM-plotter. The number of patients in the dataset were 655 and $p = 0.00043$. (**E**) ETS1 expression is upregulated in mesenchymal-like ovarian cancer patient tumors. Relative ETS1 expression (log2) in TCGA ovarian serous adenocarcinoma patients ($n = 416$) binned into epithelial-like and mesenchymal-like as determined by UCSC Cancer Browser. P-value determined by student's T-test. (**F**) qPCR for CDH1 (E-cadherin), ZEB2 and FN1 (Fibronectin) were done in Kuramochi, OVCAR4, OVCAR8 and OVCAR5 cells grown on 3D culture and compared to controls grown on normal culture dishes. *$p < 0.01$, Students *t*-test.

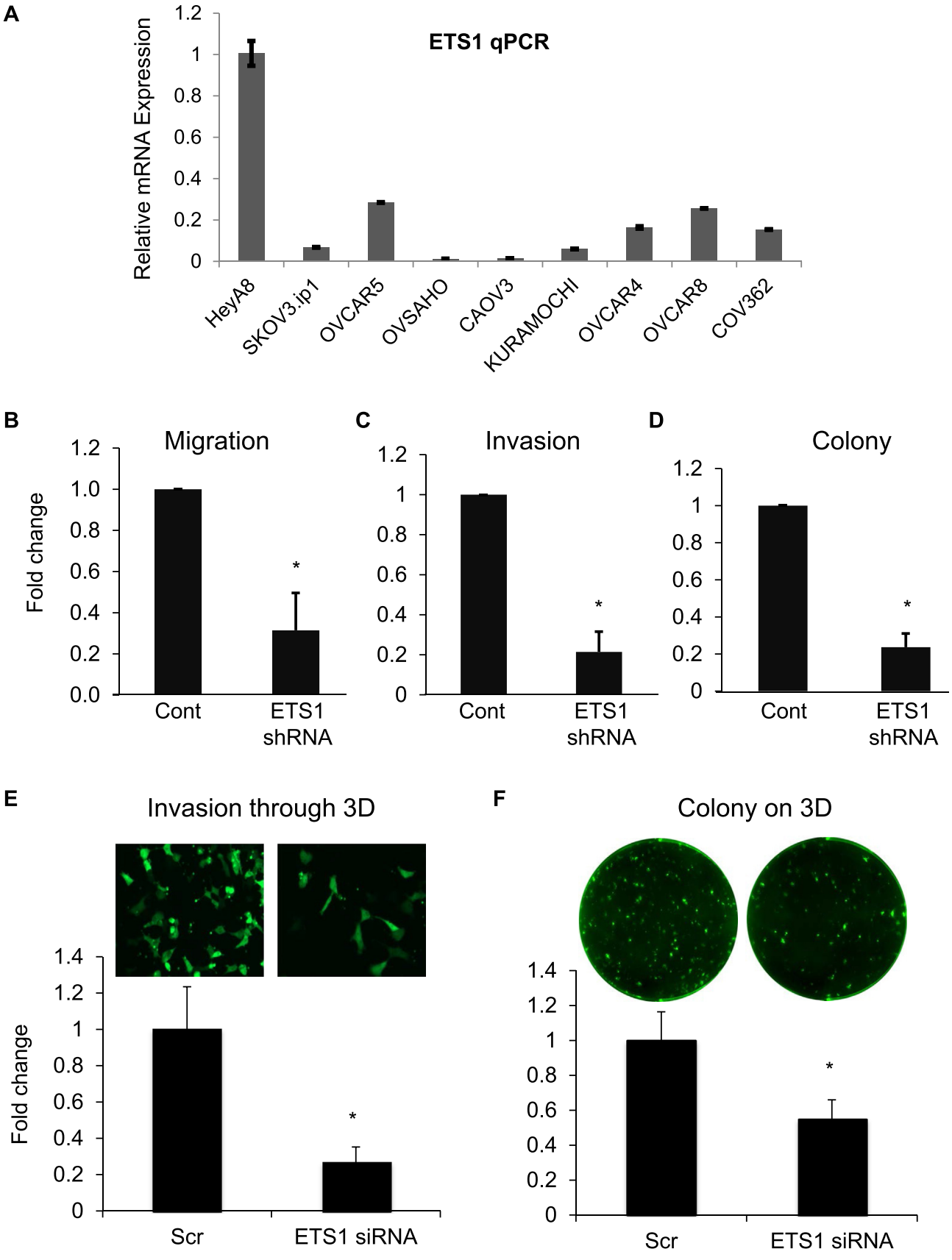
A
ETS1 qPCR
Relative mRNA Expression
1.2
1
0.8
0.6
0.4
0.2
0
HeyA8
SKOV3.ip1
OVCAR5
OVSAHO
CAOV3
KURAMOCHI
OVCAR4
OVCAR8
COV362
B
Migration
Fold change
1.2
1.0
0.8
0.6
0.4
0.2
0.0
*
Cont
ETS1 shRNA
C
Invasion
1.2
1
0.8
0.6
0.4
0.2
0
*
Cont
ETS1 shRNA
D
Colony
1.2
1
0.8
0.6
0.4
0.2
0
*
Cont
ETS1 shRNA
E
Invasion through 3D
Fold change
1.4
1.2
1
0.8
0.6
0.4
0.2
0
*
Scr
ETS1 siRNA
F
Colony on 3D
1.4
1.2
1
0.8
0.6
0.4
0.2
0
*
Scr
ETS1 siRNA

specific antibody for 4 h at 4 °C, washed, and DNA isolated by phenol/chloroform. Antibodies used in ChIP were from Santa Cruz Biotechnology: anti-ETS1 (Santa Cruz Cat# SC-350). Library preparation and data analysis was carried out as previously described [25]. Data validation was done using ChIP-qPCR with primers listed in Supplementary Fig. 1.

2.15. RNA sequencing and analysis

Total RNA for three independent biological replicates was isolated from HeyA8 cells transduced with lentiviral shRNA knockdown vectors using the miRNeasy mini kit (Qiagen) according to manufacturer's instructions. Sequencing libraries for whole transcriptome analysis were generated using a modified Illumina TruSeq sample preparation protocol as described previously [26]. The sequencing was performed by the Indiana University Center for Genomics and Bioinformatics core facility using an Illumina TruSeq.

2.16. Immunofluorescence

The 3D culture was assembled on polyD-lysine coated glass coverslips and OC cells expressing GFP or RFP were seeded on the 3D culture or on the cover slips. At end point, cells were fixed with 4% paraformaldehyde and permeabilized, blocked, and probed with primary antibodies against ETS1, FAK, p-p44/42 MAPK and p44/42 MAPK (Santa Cruz Cat# SC-350, Cell Signaling Cat# 3285, 4370 and 4695 respectively). Alexa Fluor 488 or 594 tagged secondary antibodies (Cell Signaling Cat# 44125 and ThermoFisher Cat# A11039) were used for detection and the nuclei were stained with Hoechst 33342 (ThermoFisher Cat# H3570) and the coverslips were mounted with ProLong Gold (ThermoFisher Cat# P36934) and imaged using a Leica SP8 confocal microscope.

2.17. Immunoblotting

Immunoblotting was done as previously described [20]. Briefly, proteins were separated by 4–20% gradient SDS-PAGE and transferred to nitrocellulose, probed with anti-ETS1 (Santa Cruz Cat# SC-350), phospho-FAK (T397) or FAK antibody (Cell Signaling Cat# 8556S and 3285S) and detected using a HRP-linked anti-mouse or anti-rabbit IgG secondary antibody (Cell Signaling, Cat# 7076, 7074). Actin (Sigma Cat# #G9295) was probed as a loading control.

2.18. Treatment with U0126

The cells were treated with 10 μM U0126 (Cell Signaling Cat# 9903S) to inhibit p44/42 MAP kinase. Control cells were treated with DMSO. Cells were lysed for immunoblotting or fixed for imaging at indicated times.

2.19. TCGA data analysis for ETS1 and PTK2 expression

FPKM values for genes ETS1 (ENSG00000134954) and PTK2 (ENSG00000169398) were extracted from gene expression dataset comprising of 379 ovarian cancer patient samples downloaded from “Genomic Data Commons Data Portal” (https://portal.gdc.cancer.gov/). Samples were ordered on ETS1 expression values and were grouped into three parts, each containing a third of the samples (~127). Samples with ETS1 FPKM less than 2.89 went into first tertile and those with ETS1 FPKM greater than 4.85 went into the third tertile while those in the middle went into second tertile. PTK2 FPKM values for samples from first and third tertiles were plotted as box plots.

2.20. Statistics

Data analysis was done by unpaired, two-tailed Student's t-test assuming equal variance of the test and the control populations.

3. Results

3.1. ETS1 is the most upregulated oncogenic ETS in OC metastatic colonization

We have recapitulated the early events on metastatic colonization using an organotypic 3D culture model mimicking the outer layers of the human omentum [10] (Fig. 1A). Briefly, normal omental fibroblasts (NOFs) and human primary mesothelial cells (HPMCs) were isolated from omentum samples obtained from female donors undergoing abdominal surgeries for non-cancer conditions. The NOFs were mixed with collagen 1 and seeded first in the culture dishes. They were overlaid with a confluent monolayer of HPMCs from the same patient. Together, this mimics the outer mesothelium covering the omentum and the underlying basement membrane. The GFP labeled ovarian cancer cells (OVCAR8, KURAMOCHI and HeyA8) were seeded on the 3D culture 24 h later. The ovarian cancer cells were isolated 2 days

Fig. 2. ETS1 inhibition decreases motility and clonogenic growth. (**A**) qPCR for ETS1 in a panel of OC cell lines to determine its baseline expression levels. ETS1 was stably knocked down in HeyA8 cells, which were then compared with cells with shRNA against luciferase as controls in various assays. (**B**) The effect of knocking down ETS1 was tested using a transwell migration assay. Cells were seeded in transwell inserts with 8 μm pores and allowed to migrate towards the chemottractant (medium with 10% FBS). The migrated cells were fixed, stained, imaged and counted (mean ± SD; 3 independent experiments). (**C**) ETS1 silenced HeyA8 cells were seeded in transwell inserts coated with growth factor reduced matrigel and allowed to invade towards medium containing 10% FBS. Invaded cells were fixed, stained, imaged and quantified (mean ± SD; 3 independent experiments). (**D**) HeyA8 cells with stable knock down of ETS1 were seeded in 6 well plates for colony formation assay. The colonies were fixed, stained and counted (mean ± SD; 3 independent experiments). (**E**) The omental 3D culture was assembled in fluoroblock transwell inserts and the ETS1 silenced HeyA8GFP cells were allowed to invade through the 3D culture to better mimic the initial invasion through the outer layers of the omentum. The invaded GFP expressing cells were imaged, counted and plotted. Representative images of the invaded GFP expressing HeyA8 cells are shown above the respective bars (mean ± SD; 3 independent experiments). (**F**) HeyA8GFP cells were seeded to form colonies on the omental 3D culture grown in 6 well plates to replicate early colonization of the omentum *in vitro*. The fluorescent green colonies formed were imaged and counted. Respective images of the colonies are shown above the bars (mean ± SD; 3 independent experiments). *$p < 0.01$, Students *t*-test. (For interpretation of the references to colour in this figure legend, the reader is referred to the web version of this article.)

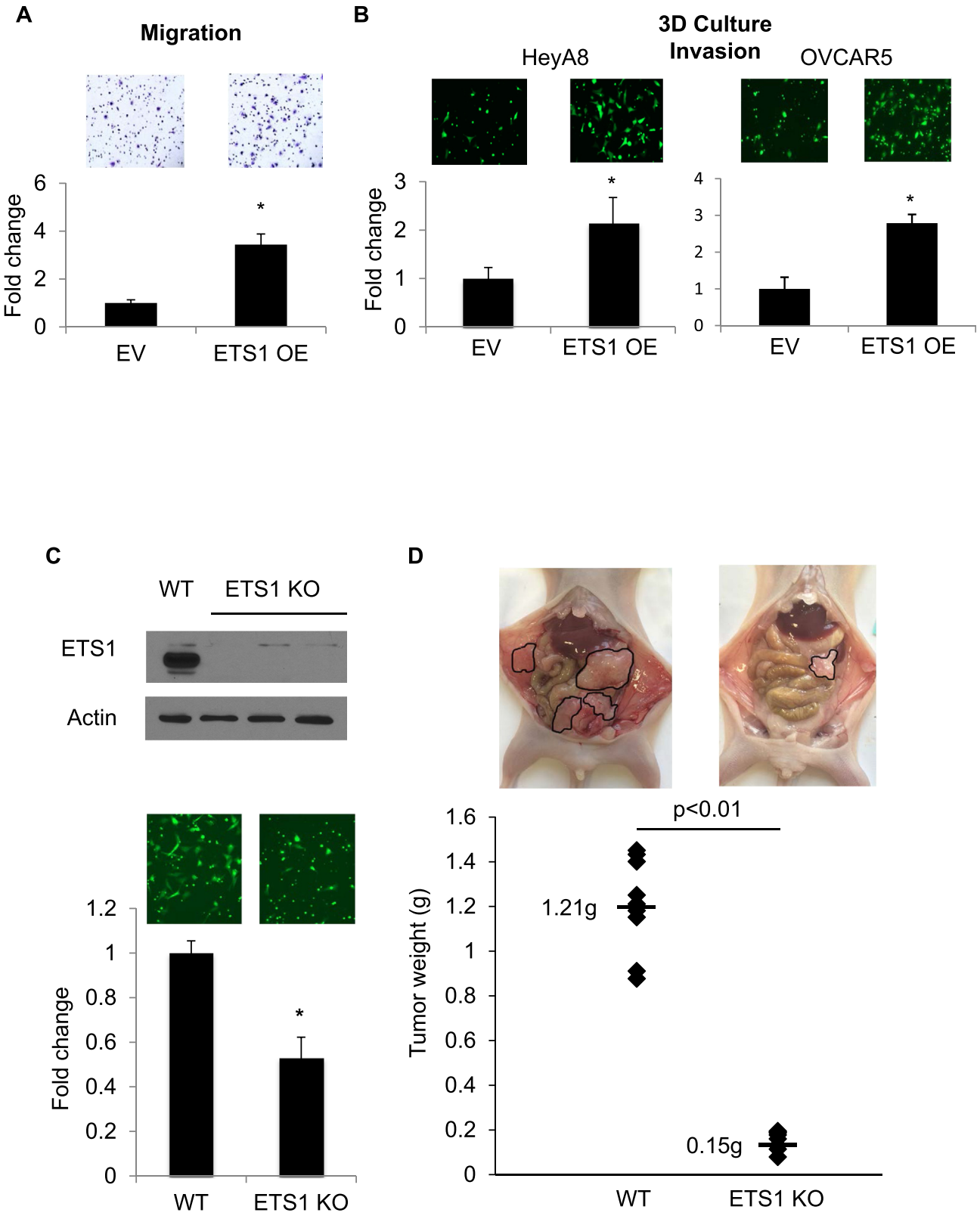
A
Migration
Fold change
6
4
2
0
*
EV
ETS1 OE
B
3D Culture Invasion
HeyA8
OVCAR5
Fold change
3
2
1
0
*
EV
ETS1 OE
4
3
2
1
0
*
EV
ETS1 OE
C
WT
ETS1 KO
ETS1
Actin
Fold change
1.2
1
0.8
0.6
0.4
0.2
0
*
WT
ETS1 KO
D
p<0.01
Tumor weight (g)
1.6
1.4
1.2
1
0.8
0.6
0.4
0.2
0
1.21g
0.15g
WT
ETS1 KO

later using fluorescence activated cell sorting. We measured the mRNA levels of various ETS factors previously implicated in cellular migration and invasion (ETS1, ETS2, ETV1, ETV4, ETV5, ERG, FLI1 and FEV) in these OC cells by qPCR. ETS1 was found to be the most commonly upregulated among these ETS factors in the OC cells seeded on the 3D culture (Fig. 1B and Supplementary Fig. 3A). OC cells seeded on HPMCs alone also demonstrated a similar increase in ETS1 expression (Supplementary Fig. 3B). Therefore, we concluded that the interactions of the OC cells with the mesothelial cells were sufficient to trigger an increase in ETS1 expression in the OC cells. Thereafter, we compared ETS1 expression levels in ovarian cancer patient tumors, which were chemo-naïve to that of normal fallopian tubes since most high-grade serous ovarian cancer originates from the fallopian tube [27]. Immunohistochemical staining for ETS1 in an OC tissue microarray revealed a significant increase in ETS1 expression in ovarian tumors relative to normal fallopian tubes (Fig. 1C). An analysis of the effect of ETS1 overexpression on prognosis in OC patients was done using the KM-plotter database [28,29]. Overexpression of ETS1 resulted in decreased 5-year survival of OC patients (Fig. 1D) with the median survival being 36 months for high ETS1 expression compared to 50.97 months for low ETS1 expression. No significant difference was noted for ETS2 and ETV1 (Supplementary Fig. 4).

We next used the data from The Cancer Genome Atlas (TCGA) [14] to test if ETS1 levels in tumors correlated with epithelial-mesenchymal transition (EMT). Tumors were separated into epithelial and mesenchymal groups based on EMT score [30] and ETS1 expression levels were compared between groups. Tumors with higher mesenchymal gene expression also had significantly higher levels of ETS1 compared to ovarian tumors with a more epithelial gene signature (Fig. 1E). Therefore, ETS1 potentially regulates or is associated with a gene expression program that correlates with an EMT phenotype. To confirm this in our system, the expression of the epithelial marker E-cadherin (CDH1) and the mesenchymal markers Zeb2 and fibronectin (FN1) was analyzed by qPCR in Kuramochi, OVCAR4, OVCAR8 and OVCAR5 cells seeded on the 3D culture (Fig. 1F). The mesenchymal markers were found to be markedly increased in the OC cells upon interaction with the 3D culture while E-cadherin remained unchanged in Kuramochi and OVCAR4 but increased slightly in OVCAR8 and OVCAR5. This reflects the complex regulation of the EMT phenotype and indicates that ETS1 may be one of many regulators involved. Since a mesenchymal phenotype favors OC metastasis to the omentum [31] we proceeded to investigate the role ETS1 in OC metastasis.

3.2. ETS1 plays an important role in metastasis

Having observed an increase in ETS1 expression in OC cells interacting with mesothelial cells and that ETS1 overexpression correlates with poor outcome in OC patients, we proceeded to investigate the functional effects of ETS1 on OC cells. As the OC cells attach to the mesothelium covering the omentum, they need to invade and proliferate to establish the metastatic colonies so we tested motility, invasiveness and clonogenic growth. In order to determine the OC cell lines to be used for silencing or overexpressing ETS1, we profiled ETS1 expression levels in a panel of OC cell lines (Fig. 2A). HeyA8 and OVCAR5 have high and intermediate levels of expression of ETS1 and they perform very robustly in functional assays [22] and were selected for the subsequent experiments. Transient silencing of ETS1 in HeyA8 and OVCAR5 OC cells resulted in a decrease in their migration, invasion and colony formation (Fig. 2 B–D and Supplementary Fig. 5). To test the effect of ETS1 on OC metastasis *in vitro,* ETS1 was silenced in GFP expressing HeyA8 cells, which were then allowed to invade through the omental 3D culture assembled in fluoroblock transwell inserts. This effectively mimicked the attachment and subsequent invasion of OC cells through the outer layers of the omentum. The invaded GFP expressing cells were imaged and counted. ETS1 knock down resulted in a decrease in the ability of HeyA8 cells to invade through the 3D culture (Fig. 2E). Similarly, ETS1 was silenced in GFP expressing HeyA8 cells, which were allowed to colonize 3D omental cultures assembled in 6 well plates. The fluorescent colonies formed were imaged and quantified. Knocking down ETS1 decreased their ability to form colonies on the 3D culture (Fig. 2F). Silencing was confirmed with qPCR and western blotting (Supplementary Figs. 6A and B). Taken together, the above data indicated that depleting the endogenous levels of ETS1 in OC cells resulted in a decrease in their functions that are necessary for colonizing the metastatic site like motility, invasiveness and growth. More importantly, using the 3D organotypic culture, these decreased functions were also recapitulated in OC cells undergoing early metastatic events.

We next proceeded to test the functional effects of overexpressing ETS1 in OC cells. Transient overexpression of ETS1 in OVCAR5 OC cells resulted in an increase in their *trans*-well migration (Fig. 3A). GFP expressing HeyA8 and OVCAR5 cells were transiently transfected with an ETS1 overexpression vector and were allowed to invade through 3D omental cultures assembled in fluoroblock *trans*-well inserts. The fluorescent invaded cells were imaged and quantified. Overexpression of

Fig. 3. ETS1 promotes OC metastasis. (**A**) ETS1 was transiently overexpressed in OVCAR5 cells (ETS1 OE) which were then seeded in transwell inserts with 8 μm pores and their ability to migrate was compared to vector control cells (EV). The migrated cells were imaged and quantified. Representative images of migrated cells are shown above respective bars (mean ± SD; 3 independent experiments). (**B**) The ability of ETS1 overexpressing HeyA8GFP (left) and OVCAR5 (Right) cells to invade through the 3D omentum culture assembled in fluoroblock transwell inserts were compared with vector control cells. The fluorescent green invaded cells were imaged and counted. Representative images of the invaded cells are shown above the respective bars (mean ± SD; 3 independent experiments). (**C**) *Top:* ETS1 was knocked out in HeyA8 cells (ETS1 KO) using CRISPR/Cas9 and immunoblotting for ETS1 protein expression was done with the clones to confirm knockout. *Bottom:* ETS1 KO HeyA8 cells were allowed to invade through the 3D omentum culture and the invaded cells were imaged and quantified (mean ± SD; 3 independent experiments). (**D**) Mouse xenograft model of OC metastasis was used to test the effect of ETS1 KO on OC metastasis. HeyA8 cells with ETS1 knocked out (ETS1 KO) or wild type controls (WT) were injected intraperitoneally in 6-week-old female athymic nude mice (n = 9 mice/group). Mice were euthanized after 15 days and the tumors surgically removed and weighed. The tumor weight was plotted with the mean values indicated alongside. Representative images of tumor bearing mice are shown above respective groups. $^{*}p < 0.01$, Students *t*-test. (For interpretation of the references to colour in this figure legend, the reader is referred to the web version of this article.)

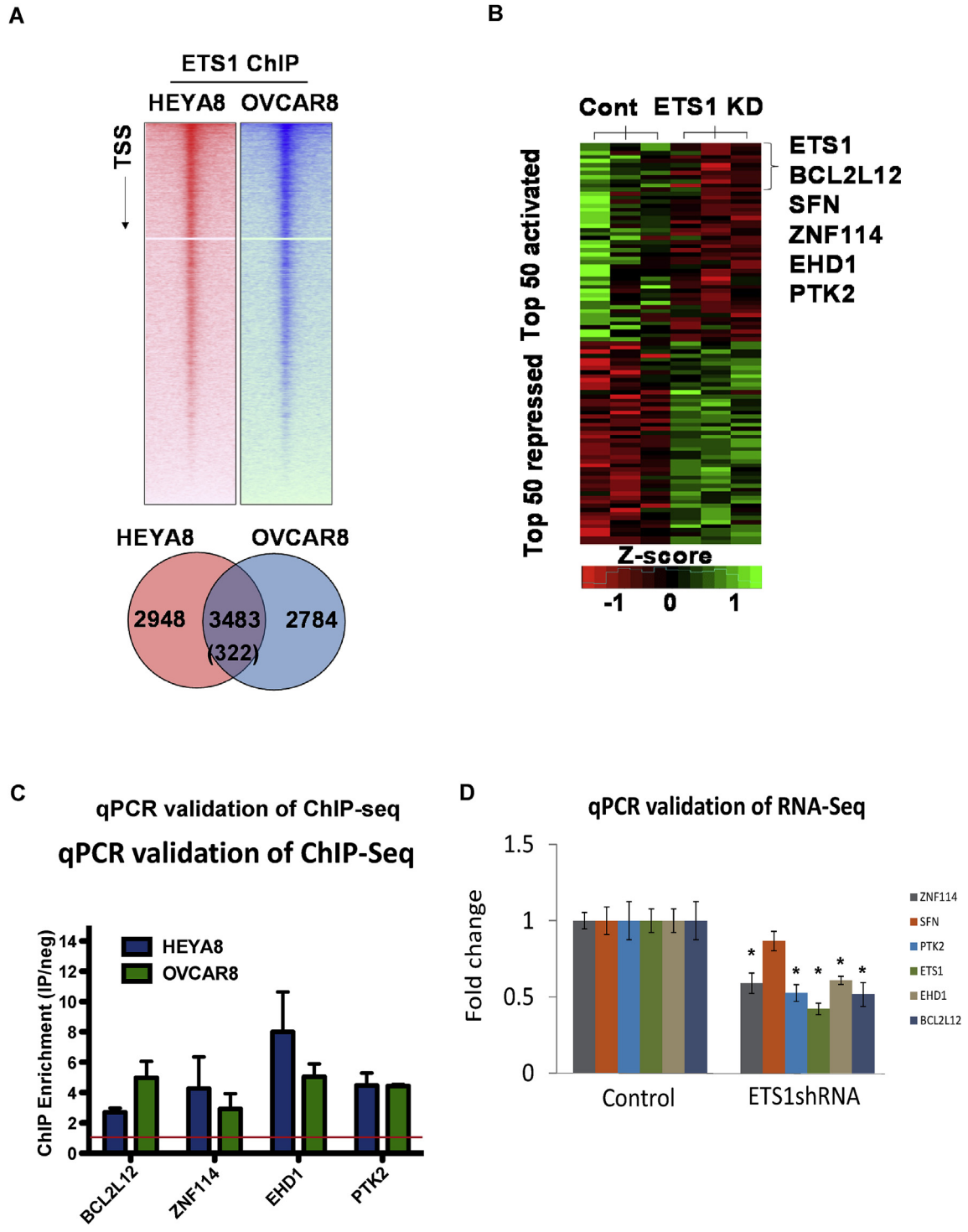

Fig. 4. Determination of transcriptional targets of ETS1 in OC. (**A**) *Top:* ChIP-seq data presented as a heat map of ETS1 enrichment at transcriptional start sites (TSS) genome wide, as determined by NGSPlot. *Bottom:* Venn diagram of all overlapping bound regions (promoter and enhancer) between ETS1 in HEYA8 and OVCAR8 ovarian cancer cell lines. Number in parenthesis indicated number of bound regions as expected by random chance, based on estimate of 125,000 possible regions of open chromatin. (**B**) Heat map of relative RPKM values determined by RNA-seq differential expression analysis and created by cummeRbund (red = low expression, green = high expression). Top 50 genes activated by ETS1 and repressed by ETS1 are shown along with three biological replicates. Z-score scale from −1 to 1 used to determine intensity of red/green colors in each sample. (**C**) ChIP-qPCR was performed to validate ETS1 binding to the promoters of the top targets. (**D**) qPCR validation of the RNA-seq results for the top targets (mean ± SD; 3 independent experiments) $^{*}p < 0.01$ compared to respective control.

Table 1
Most over-represented ontologies of 289 genes significantly changed upon ETS1 knockdown.

Ontology	*P*-value
Regulation of cell migration	2.2×10^{-11}
Positive regulation of developmental process	1.1×10^{-8}
Regulation of cell proliferation	1.6×10^{-8}
Anatomical structure formation	1.6×10^{-7}
Regulation of response to stimulus	2.9×10^{-7}

ETS1 resulted in increased invasion through the 3D culture (Fig. 3B). Overexpression was confirmed by western blotting (Supplementary Fig. 7A). Having confirmed that ETS1 is functionally relevant for OC metastasis *in vitro*, we next tested the role of ETS1 in OC metastasis *in vivo* using a mouse xenograft model of OC metastasis. ETS1 was knocked out in HeyA8 cells (HeyA8 ETS1 KO) using CRISPR-Cas9 (Fig. 3C (top), Supplementary Fig. 2) and the functional effects of its knockout were confirmed with invasion through the 3D culture (Fig. 3C, bottom). HeyA8 ETS1 KO or wild type control HeyA8 cells (1×10^6 cells) were injected intraperitoneally in female athymic nude mice (9 mice per group). Mice were euthanized 15 days after injecting the cancer cells and the tumors were surgically removed and weighed. Knocking out ETS1 resulted in a significant decrease in metastatic tumors in the mice (Fig. 3D).

3.3. ETS1 drives OC metastasis phenotypes through its transcriptional target PTK2

To identify direct targets of ETS1 that might be responsible for its functional effects, ETS1 ChIP-seq was done in both HeyA8 and OVCAR8 cells. Comparison of ETS1 binding across all promoter regions in these two cell lines showed strikingly similar profiles (Fig. 4A). In total, ETS1 bound 6431 regions in HeyA8 cells and 6267 regions in OVCAR8. Among them, 3483 regions were in common, a greater than 10-fold enrichment over the random prediction (Fig. 4A). These data indicate that the ETS1 cistrome is conserved across multiple ovarian cancer cell lines. In a parallel approach, ETS1 was stably knocked down in HeyA8 cells and the gene expression levels in these cells were compared with the vector control cells using mRNA-seq. 289 genes had significant changes in gene expression ($P < 0.01$) (Supplemental Table S1). Ontology analysis of these 289 genes revealed that the most over-represented function was “Regulation of cell migration” (Table 1), consistent with our finding in Fig. 2B, and with the EMT signature in OC TCGA data (Fig. 1E). Of the 289 genes that change expression after ETS1 knockdown in HeyA8 cells, 97 had a neighboring ETS1-bound region in HeyA8 cells, and 54 had the same region bound by ETS1 in OVCAR8 cells (Supplementary Table S1). From these 54 genes, we then selected the five (excluding ETS1 itself) that decreased the most upon ETS1 knockdown for further analysis (Fig. 4B). ChIP enrichment and decreased expression of these genes upon ETS1 knockdown were then validated by quantitative PCR (Fig. 4C and D).

Among these top five targets of ETS1 in ovarian cancer cells was protein tyrosine kinase 2 (*PTK2*), which codes for focal adhesion kinase (FAK), a protein involved in processes essential for invasion and metastasis [32–34]. We and others have previously demonstrated the role of FAK in ovarian cancer metastasis to the omentum [10,35–37]. To confirm the downregulation of FAK at the protein level, immunoblotting was done using protein lysates from ETS1 KO OC cells. We observed a decrease in FAK protein expression in ETS1 KO cells (Fig. 5A). Immunofluorescence imaging of FAK in these cells indicated that ETS1 was only involved in regulating the expression and not the distribution of FAK (Fig. 5B). Thereafter, we tested if knocking down FAK (Supplementary Fig. 7B) in OC cells could phenocopy the functional effects of knocking down ETS1. Silencing FAK resulted in decreased migration and proliferation (Fig. 5C and D). This indicated that loss of FAK had similar effects on the OC cells as the loss of ETS1. To confirm that FAK was functioning downstream of ETS1, a functional rescue experiment was performed. FAK was overexpressed in ETS1 KO cells followed by migration assay. As expected, the ETS1 KO cells decreased migration compared to the WT cells and overexpression of FAK in the ETS1 KO cells reverted the migration levels back to the WT levels (Fig. 5E). Similar effects were observed for colony formation (Supplementary Fig. 8). These results implicate FAK as a downstream effector of ETS1 during ovarian cancer metastasis to the omentum. We also analyzed the expression levels of ETS1 and PTK2 in the ovarian cancer TCGA data and PTK2 expression was significantly higher in tumors with high ETS1 expression (Fig. 5F). To better understand the mechanism of transcriptional regulation of PTK2 by ETS1, the ETS1 bound regions of the PTK2 promoter was analyzed in HeyA8 and OVCAR8 using our ChIP-seq data showing common binding sites as well as cell type specific binding (Fig. 5G).

3.4. ETS1 expression is regulated by activation of MAP kinase signaling induced by the microenvironment

We next attempted to identify the mechanism of regulation of ETS1 in the metastasizing OC cells when they interact with the mesothelial cells. ETS1 has been reported to be phosphorylated by p44/42 mitogen activated protein kinase (MAPK) at its T38 and S41 residues, which increases its activity by enhancing its affinity for the co-activator CBP/p300 [38,39]. Since ETS1 can also regulate its own transcription, this can potentially lead to increased ETS1 expression. Therefore, we treated OC cells with U0126, which inhibited p44/42 MAPK signaling (Supplementary Fig. 9A) causing a decrease in ETS1 protein expression and phosphorylation (Fig. 6A) as well as ETS1 mRNA levels (Supplementary Fig. 9A). It also decreased FAK expression (Supplementary Fig. 9A). We then tested the effect of inhibition of p44/42 MAPK signaling in OC cells seeded on the 3D culture. A significant decrease in ETS1 expression in the OC cells was observed upon p44/42 MAPK inhibition in OC cells seeded on 3D culture compared to controls (Fig. 6B). Moreover, increased phosphorylation of p44/42 MAPK was observed in OC cells seeded on the 3D culture compared to controls (Fig. 6C). However, the total p44/42 MAPK protein levels remained unaffected by the interactions with the 3D culture (Supplementary Fig. 9C). Thereafter, we proceeded to investigate the functional effects of p44/42 MAPK inhibition on the ability of the OC cells to migrate. Treatment with U0126 inhibited migration and mimicked the effects of ETS1 knock down. However if the cells were transfected with a constitutively active ETS1 (T38E or T38E and S41E) (Supplementary Fig. 9B), it rescued the cells from the effects of MAPK inhibition on migration (Fig. 6D). Taken together, this indicates that the activation of p44/42 MAPK signaling in the OC cells interacting with the mesothelial cells that cover the omentum leads to the activation and overexpression of ETS1. The ETS1 overexpression leads to increased FAK levels, which helps the OC cells to invade into the omentum and form the metastatic tumor (proposed model in Fig. 6E).

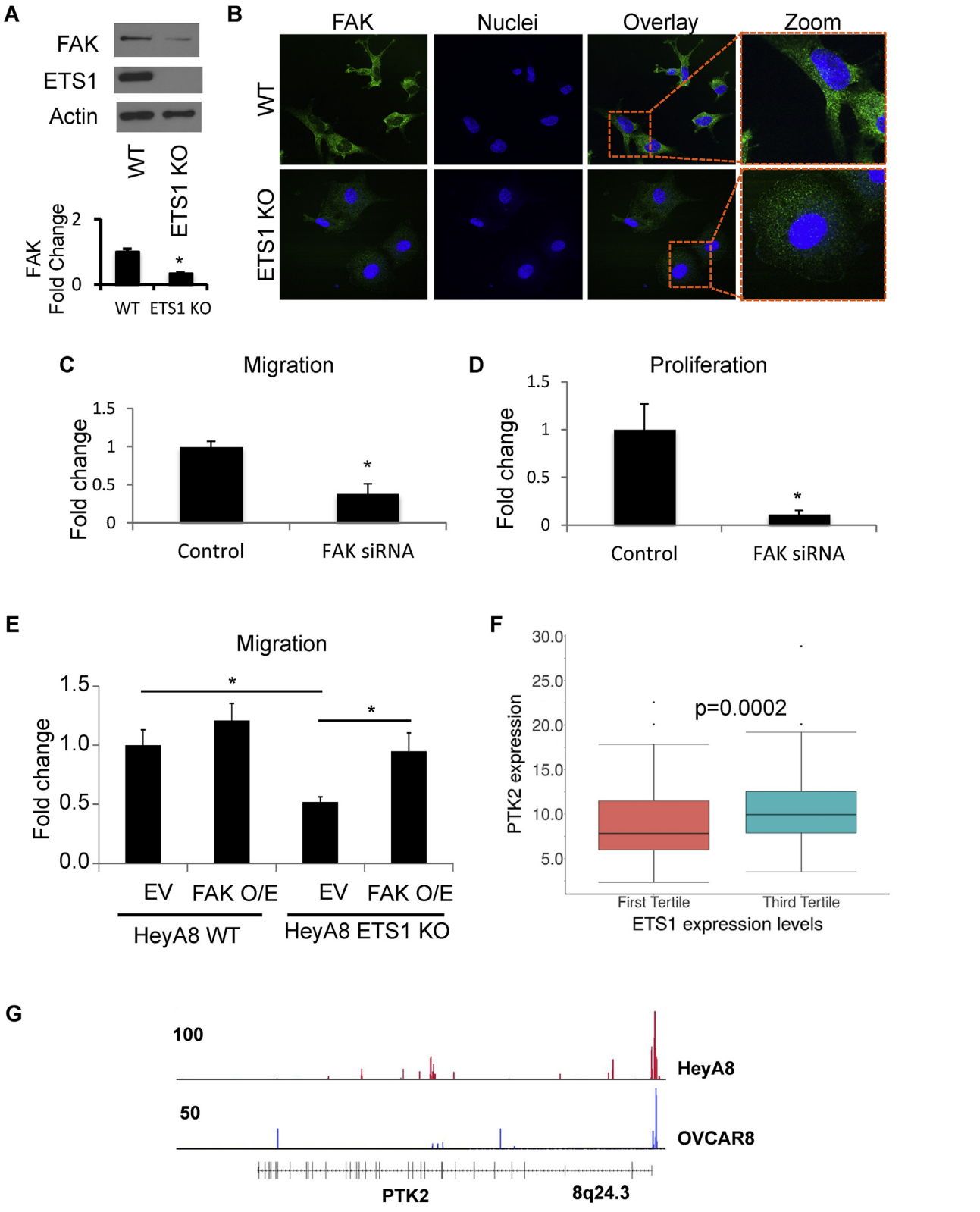

Fig. 5. FAK is the functional effector of ETS1 in OC. (**A**) Immunoblot for FAK in ETS1 knockout (ETS1 KO) HeyA8 cells compared to the wild type (WT) control. Quantification of FAK expression normalized to actin is plotted below. (**B**) Immunofluorescence analysis of FAK (green) expression in ETS1 knockout (ETS1 KO) HeyA8 cells compared to the wild type (WT) control. Nuclei are stained with Hoechst 33342. (**C**) Transwell migration assay was performed with OVCAR5 cells transiently transfected with FAK siRNA or scrambled control. The migrated cells were imaged and quantified (mean ± SD; 3 independent experiments). (**D**) OVCAR5 cells were transfected with FAK siRNA or scrambled control and were used to perform a proliferation assay (mean ± SD; 3 independent experiments). (**E**) FAK was transiently overexpressed in ETS1 knockout (ETS1 KO) or wild type (WT) HeyA8 cells and these cells were subjected to transwell migration with medium containing 10% FBS serving as the chemottractant. Migrated cells were imaged and quantified (mean ± SD; 3 independent experiments). (**F**) Plot comparing the expression of PTK2 in tumors segregated into 1st and 3rd tertiles on the basis of their ETS1 expression levels from the ovarian cancer TCGA gene expression data (n = 379). (**G**) ETS1 occupancy at the PTK2 promoter is plotted by -log binomial *P*-value from ChIP-seq data of HeyA8 and OVCAR8 OC cells. *p < 0.01 compared to respective control. (For interpretation of the references to colour in this figure legend, the reader is referred to the web version of this article.)

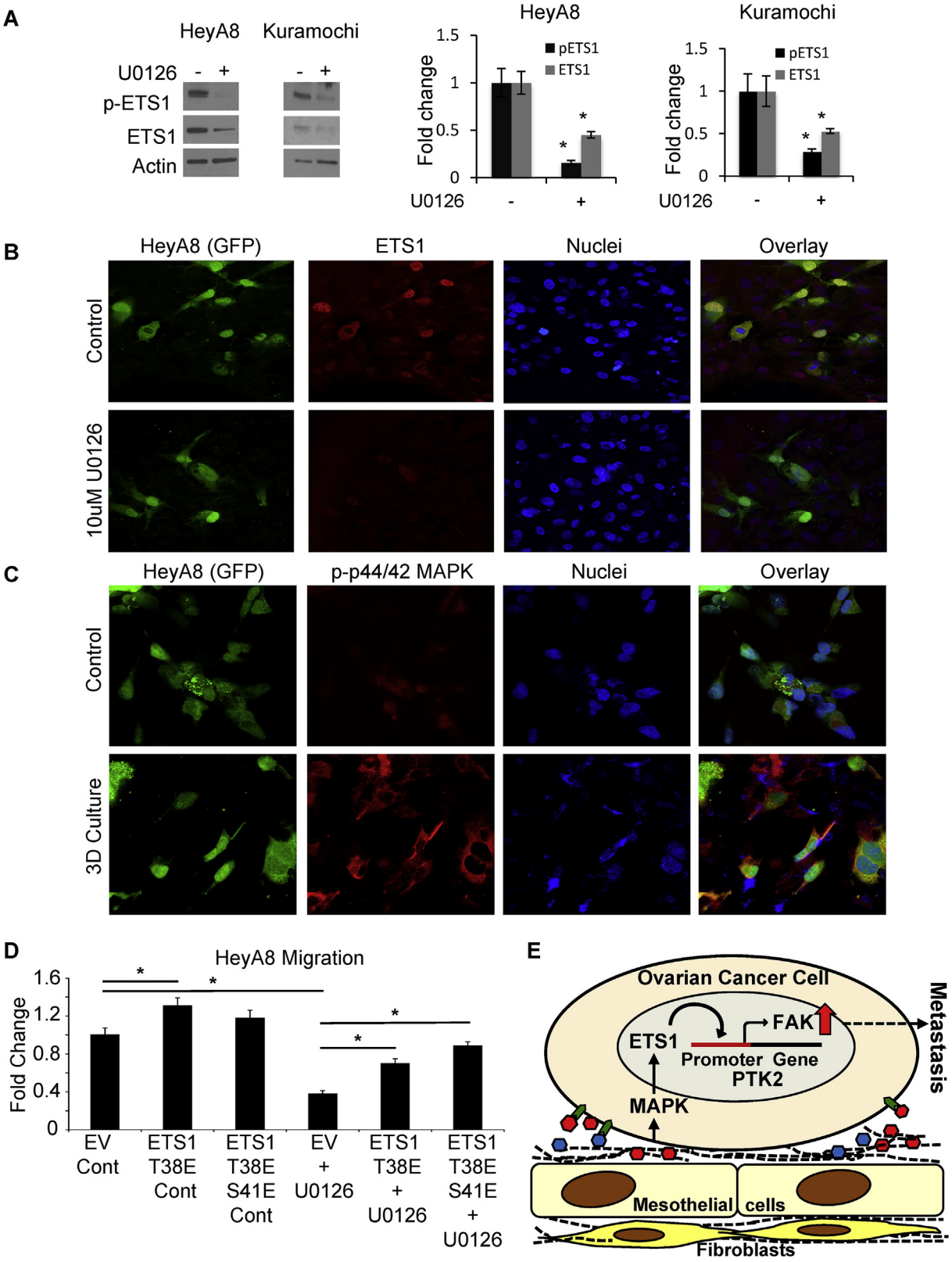

Fig. 6. MAP kinase signaling induced by the microenvironment upregulates ETS1. (**A**) Left: HeyA8 or Kuramochi cells were treated with 10 μM U0126 or DMSO and cells were lysed after 48 h of treatment. Immunoblotting for phosphorylated ETS1 (pETS1) and total ETS1 was performed using the lysates. Right: Quantification of the western blots for pETS1 and ETS1 normalized to actin for each cell is provided for the respective blots. (**B**) HeyA8GFP cells were seeded on the 3D omentum culture and treated with 10 μM U0126 or DMSO for 48 h and then fixed and immunostained for ETS1 (red) and nuclei were stained with Hoechst 33342 to reveal the normal cells of the 3D culture. (**C**) HeyA8GFP cells were seeded on the 3D omentum culture for 48 h and then fixed and immunostained for phosphorylated p44/42 MAPK (red) and nuclei were stained with Hoechst 33342. (**D**) HeyA8 cells were transiently transfected with constitutively active ETS1 (ETS1 T38E or ETS1 T38E S41E) which were then treated with 10 μM U0126 or DMSO and used for transwell migration assay. Error bars represent mean ± SD; 3 independent experiments. (**E**) Proposed model: Upon interactions with the mesothelial cells covering the omentum, MAPK pathway is activated in the metastatic OC cells. This results in the activation and increased transcription of ETS1 which upregulates the transcription of its target PTK2. PTK2 codes for FAK, which promotes the initial invasiveness and growth, needed for metastatic colonization. *$p < 0.01$ compared to respective control.

4. Discussion

The roles of the tumor microenvironment and the microenvironment of the metastatic site have increasingly come into focus over the recent years as key determinants of successful metastasis [40]. With the use of 3D culture models, we and others have demonstrated the molecular mechanisms involved in the cross-talk between cancer cells and the microenvironment during early metastatic colonization of OC to the omentum [6,20,41–43]. However, little is known about pro-metastatic gene expression changes induced by transcription factors activated via interaction with the metastatic microenvironment. Using an organotypic 3D culture model that mimics the surface layers of the omentum, we report here the upregulation of ETS1 as a result of interaction of the cancer cells with the mesothelial cells that cover the omentum (Fig. 1). Analysis of published OC patient datasets using KM-plotter showed an increased ETS1 expression led to poor prognosis in OC patients (Fig. 1). We also found an increased ETS1 protein expression in TMAs of OC tumors compared to normal fallopean tubes (Fig. 1). ETS1 was found to be functionally important for metastatic colonization *in vitro* as well as in mouse xenografts (Figs. 2 and 3). The key transcriptional target was identified as PTK2 which codes for FAK and was found to be responsible for the increased invasiveness/motility and growth (Fig. 5). ETS1 was found to be regulated in the OC cells by the activation of MAP kinase signaling triggered by their interactions with the mesothelium covering the metastatic site (Fig. 6).

Increased ETS1 mRNA expression has been corelated with poor prognosis in OC [18]. Increased transcription of several extracellular proteases by ETS1 has been shown to promote invasion in ovarian cancer [13,44]. Our studies for the first time report the increased expression of ETS1 in the metastasizing OC cells upon productive interactions with the microenvironment of the metastatic site. It further revealed that this microenvironment induced increase in ETS1 played a significant role in metastatic colonization.

Our approach of a combination of RNA-seq of ETS1 silenced OC cells and ChIP-seq revealed its direct targets in ovarian cancer (Fig. 4). *PTK2* which codes for FAK was identified as a novel target regulated by ETS1. Upon attaching to the omentum, the metastasizing OC cells need to invade through the mesothelium and the underlying basement membrane in order to subsequently establish the metastatic colonies. FAK is known to be a key promoter of invasion and interactions with the ECMs present in the basement membrane [10,45]. Therefore, we decided to focus on PTK2 among the top targets of ETS1. While ETS1 has been reported to promote breast cancer metastasis through β_1-integrin mediated FAK/SRC/AKT signaling [46], we are the first to report *PTK2* as a direct transcriptional target of ETS1. FAK has been previously demonstrated to play an important role in ovarian cancer metastasis as a downstream signaling pathway induced by $\alpha_5\beta_1$-integrin when the metastsizing OC cells interact with fibronectin secreted by mesothelial cells [10,35]. Similarly, sufficient activation of FAK is deemed essential for successful metastatic colonization of breast cancer cells in the lungs [32]. It has been reported as a potential theraputic target in several cancers [47–49]. The OC cells attempting to colonize the metastatic site need to initially invade through the mesothelium and potentially through the basement membrane. An increased expression of FAK can facilitate this process and is key to successful colonization. Overexpression of FAK rescued the reduced migration in ETS1 KO cells (Fig. 5D) which demonstrated that FAK is a functional mediator of ETS1 during OC metastasis. This reveals a novel mechanism of increased expression of FAK as a result of ETS1 induction by the microenvironment. The increased amounts of FAK can be activated by the integrin mediated signaling triggered by the OC cells invading through the ECM of the basment membrane of the omentum during early metastatic colonization [10,47].

Our data demonstrated that the interaction of the OC cells with the mesothelial cells activated MAPK signaling, which led to the upregulation of ETS1. This agrees with the reported mechanism of ETS1 activation by MAPK signaling which increases its own transcription [25]. MAPK signaling is activated in metastatic serous OC and is reported to promote metastasis [50,51]. It has been shown to be activated in the metastasizing OC cells and other cancer cells by TGFβ, which is abundantly present in the metastatic microenvironment [39,52–54]. These can be potential mechanism of the cross-talk of the cancer cells with the mesothelium. However, this is the first report of an induction of ETS1 by MAPK activation through productive interactions with the metastatic microenviroment, which is an important mechanism to allow OC cells to establish metastases. Of note, our study accesses the role of the microenvironment in the initial steps of colonization and future studies need to focus on subsequent critical steps including induction of angiogenesis and metabolic reprogramming and the effects of hypoxia as the metastatic tumor grows in size. Similarly, the role of other ETS1 targets and their potential combanitorial effects on metastasis need to be studied in the future.

It is well documented that metastatic colonization is the rate limiting step of metastasis [8]. Disrupting the adaptive responses induced in the metastatic OC cells through their productive interactions with the omental microenvironment is a potentially promising approach to treat metastatic disease. This approach can probably prevent reseeding of metastatic tumors or development of the residual micrometastasis into full blown metastatic tumors post debulking surgery. Therefore, targeting this pathway could potentially reduce metastatic colonization by preventing induction of ETS1. A viable alternative approach for treating metastatic OC would be to target FAK, one of the key functional mediators of ETS1.

Acknowledgments

We are indebted to all the patients for their participation in tissue collection for these experiments. We also acknowledge the help of Ram Podicheti in the analysis of the TCGA data.

Appendix A. Supplementary data

Supplementary data related to this article can be found at https://doi.org/10.1016/j.canlet.2017.11.012.

Funding sources

AKM was supported by a DoD OCRP Ovarian Cancer Academy Award (W81XWH-15-0253) and a Colleen's Dream Foundation award, PCH by an American Cancer Society Research Scholar Award (RSG-13-215-01-DMC) and JPP by Medical Sciences Doane and Eunice Wright Memorial Fellowship.

Conflicts of interest

None.

References

[1] R.L. Siegel, K.D. Miller, A. Jemal, Cancer Statistics, 2016, CA: a Cancer Journal for Clinicians, vol. 66, 2016, pp. 7–30.
[2] A.K. Mitra, Ovarian Cancer Metastasis: a Unique Mechanism of Dissemination, Tumor Metastasis, InTech, 2016, pp. 43–58.
[3] H. Naora, D.J. Montell, Ovarian cancer metastasis: integrating insights from disparate model organisms, Nature reviews, Cancer 5 (2005) 355–366.
[4] R.O. Bainer, J.T. Veneris, S.D. Yamada, A. Montag, M.W. Lingen, Y. Gilad, C.W. Rinker-Schaeffer, Time-dependent transcriptional profiling links gene expression to mitogen-activated protein kinase kinase 4 (MKK4)-mediated suppression of omental metastatic colonization, Clin. Exp. metastasis 29 (2012) 397–408.
[5] E. Lengyel, Ovarian cancer development and metastasis, Am. J. Pathol. 177 (2010) 1053–1064.
[6] M.P. Iwanicki, R.A. Davidowitz, M.R. Ng, A. Besser, T. Muranen, M. Merritt, G. Danuser, T.A. Ince, J.S. Brugge, Ovarian cancer spheroids use myosin-generated force to clear the mesothelium, Cancer Discov. 1 (2011) 144–157.
[7] S. Valastyan, R.A. Weinberg, Tumor metastasis: molecular insights and evolving paradigms, Cell 147 (2011) 275–292.
[8] A.F. Chambers, A.C. Groom, I.C. MacDonald, Dissemination and growth of cancer cells in metastatic sites, Nature reviews, Cancer 2 (2002) 563–572.
[9] H.A. Kenny, S. Dogan, M. Zillhardt, K. Mitra A, S.D. Yamada, T. Krausz, E. Lengyel, Organotypic models of metastasis: a three-dimensional culture mimicking the human peritoneum and omentum for the study of the early steps of ovarian cancer metastasis, Cancer Treat. Res. 149 (2009) 335–351.
[10] A.K. Mitra, K. Sawada, P. Tiwari, K. Mui, K. Gwin, E. Lengyel, Ligand-independent activation of c-Met by fibronectin and alpha(5)beta(1)-integrin regulates ovarian cancer invasion and metastasis, Oncogene 30 (2011) 1566–1576.
[11] K.R. Delfino, S.L. Rodriguez-Zas, Transcription factor-microRNA-target gene networks associated with ovarian cancer survival and recurrence, PLoS One 8 (2013), e58608.
[12] M. Llaurado, M. Abal, J. Castellvi, S. Cabrera, A. Gil-Moreno, A. Perez-Benavente, E. Colas, A. Doll, X. Dolcet, X. Matias-Guiu, M. Vazquez-Levin, J. Reventos, A. Ruiz, ETV5 transcription factor is overexpressed in ovarian cancer and regulates cell adhesion in ovarian cancer cells, International journal of cancer, J. Int. du cancer 130 (2012) 1532–1543.
[13] S. Ghosh, M. Basu, S.S. Roy, ETS-1 protein regulates vascular endothelial growth factor-induced matrix metalloproteinase-9 and matrix metalloproteinase-13 expression in human ovarian carcinoma cell line SKOV-3, J. Biol. Chem. 287 (2012) 15001–15015.
[14] Integrated genomic analyses of ovarian carcinoma, Nature 474 (2011) 609–615.
[15] A. Kar, A. Gutierrez-Hartmann, Molecular mechanisms of ETS transcription factor-mediated tumorigenesis, Crit. Rev. Biochem. Mol. Biol. 48 (2013) 522–543.
[16] A. Seth, D.K. Watson, ETS transcription factors and their emerging roles in human cancer, Eur. J. cancer (Oxford, Engl. 1990) 41 (2005) 2462–2478.
[17] P. Nagarajan, S.S. Chin, D. Wang, S. Liu, S. Sinha, L.A. Garrett-Sinha, Ets1 blocks terminal differentiation of keratinocytes and induces expression of matrix metalloproteases and innate immune mediators, J. Cell Sci. 123 (2010) 3566–3575.
[18] B. Davidson, R. Reich, I. Goldberg, W.H. Gotlieb, J. Kopolovic, A. Berner, G. Ben-Baruch, M. Bryne, J.M. Nesland, Ets-1 messenger RNA expression is a novel marker of poor survival in ovarian carcinoma, Clin. Cancer Res. Official J. Am. Assoc. Cancer Res. 7 (2001) 551–557.
[19] N. Takai, T. Miyazaki, M. Nishida, K. Nasu, I. Miyakawa, c-Ets1 is a promising marker in epithelial ovarian cancer, Int. J. Mol. Med. 9 (2002) 287–292.
[20] A.K. Mitra, C.Y. Chiang, P. Tiwari, S. Tomar, K.M. Watters, M.E. Peter, E. Lengyel, Microenvironment-induced downregulation of miR-193b drives ovarian cancer metastasis, Oncogene 34 (2015) 5923–5932.
[21] P.C. Hollenhorst, D.A. Jones, B.J. Graves, Expression profiles frame the promoter specificity dilemma of the ETS family of transcription factors, Nucleic acids Res. 32 (2004) 5693–5702.
[22] J. Haley, S. Tomar, N. Pulliam, S. Xiong, S.M. Perkins, A.R. Karpf, S. Mitra, K.P. Nephew, A.K. Mitra, Functional characterization of a panel of high-grade serous ovarian cancer cell lines as representative experimental models of the disease, Oncotarget 7 (2016) 32810–32820.
[23] F.A. Ran, P.D. Hsu, J. Wright, V. Agarwala, D.A. Scott, F. Zhang, Genome engineering using the CRISPR-Cas9 system, Nat. Protoc. 8 (2013) 2281–2308.
[24] P.C. Hollenhorst, M.W. Ferris, M.A. Hull, H. Chae, S. Kim, B.J. Graves, Oncogenic ETS proteins mimic activated RAS/MAPK signaling in prostate cells, Genes & Dev. 25 (2011) 2147–2157.
[25] J.P. Plotnik, J.A. Budka, M.W. Ferris, P.C. Hollenhorst, ETS1 is a genome-wide effector of RAS/ERK signaling in epithelial cells, Nucleic acids Res. 42 (2014) 11928–11940.
[26] J.P. Plotnik, P.C. Hollenhorst, Interaction with ZMYND11 mediates opposing roles of Ras-responsive transcription factors ETS1 and ETS2, Nucleic acids Res. 45 (2017) 4452–4462.
[27] R. Perets, R. Drapkin, It's totally tubular. Riding the new wave of ovarian cancer research, Cancer Res. 76 (2016) 10–17.
[28] A.M. Szasz, A. Lanczky, A. Nagy, S. Forster, K. Hark, J.E. Green, A. Boussioutas, R. Busuttil, A. Szabo, B. Gyorffy, Cross-validation of survival associated biomarkers in gastric cancer using transcriptomic data of 1,065 patients, Oncotarget 7 (2016) 49322–49333.
[29] Z. Penzvalto, A. Lanczky, J. Lenart, N. Meggyeshazi, T. Krenacs, N. Szoboszlai, C. Denkert, I. Pete, B. Gyorffy, MEK1 is associated with carboplatin resistance and is a prognostic biomarker in epithelial ovarian cancer, BMC cancer 14 (2014) 837.
[30] T.Z. Tan, Q.H. Miow, Y. Miki, T. Noda, S. Mori, R.Y. Huang, J.P. Thiery, Epithelial-mesenchymal transition spectrum quantification and its efficacy in deciphering survival and drug responses of cancer patients, EMBO Mol. Med. 6 (2014) 1279–1293.
[31] R.A. Davidowitz, L.M. Selfors, M.P. Iwanicki, K.M. Elias, A. Karst, H. Piao, T.A. Ince, M.G. Drage, J. Dering, G.E. Konecny, U. Matulonis, G.B. Mills, D.J. Slamon, R. Drapkin, J.S. Brugge, Mesenchymal gene program-expressing ovarian cancer spheroids exhibit enhanced mesothelial clearance, J. Clin. Invest. 124 (2014) 2611–2625.
[32] T. Shibue, R.A. Weinberg, Integrin beta1-focal adhesion kinase signaling directs the proliferation of metastatic cancer cells disseminated in the lungs, Proc. Natl. Acad. Sci. U. S. A. 106 (2009) 10290–10295.
[33] R.A. Bartolome, I. Garcia-Palmero, S. Torres, M. Lopez-Lucendo, I.V. Balyasnikova, J.I. Casal, IL13 receptor alpha2 signaling requires a scaffold protein, FAM120A, to activate the FAK and PI3K pathways in colon cancer metastasis, Cancer Res. 75 (2015) 2434–2444.
[34] Z. Dai, S.L. Zhou, Z.J. Zhou, D.S. Bai, X.Y. Xu, X.T. Fu, Q. Chen, Y.M. Zhao, K. Zhu, L. Yu, G.H. Yang, Z. Wang, W.Z. Wu, J. Zhou, J. Fan, Capn4 contributes to tumour growth and metastasis of hepatocellular carcinoma by activation of the FAK-Src signalling pathways, J. Pathol. 234 (2014) 316–328.
[35] C.H. Chen, M.K. Shyu, S.W. Wang, C.H. Chou, M.J. Huang, T.C. Lin, S.T. Chen, H.H. Lin, M.C. Huang, MUC20 promotes aggressive phenotypes of epithelial ovarian cancer cells via activation of the integrin beta1 pathway, Gynecol. Oncol. 140 (2016) 131–137.
[36] C.S. Leung, T.L. Yeung, K.P. Yip, S. Pradeep, L. Balasubramanian, J. Liu, K.K. Wong, L.S. Mangala, G.N. Armaiz-Pena, G. Lopez-Berestein, A.K. Sood, M.J. Birrer, S.C. Mok, Calcium-dependent FAK/CREB/TNNC1 signalling mediates the effect of stromal MFAP5 on ovarian cancer metastatic potential, Nat. Commun. 5 (2014) 5092.
[37] K.K. Ward, I. Tancioni, C. Lawson, N.L. Miller, C. Jean, X.L. Chen, S. Uryu, J. Kim, D. Tarin, D.G. Stupack, S.C. Plaxe, D.D. Schlaepfer, Inhibition of focal adhesion kinase (FAK) activity prevents anchorage-independent ovarian carcinoma cell growth and tumor progression, Clin. Exp. metastasis 30 (2013) 579–594.
[38] M.L. Nelson, H.S. Kang, G.M. Lee, A.G. Blaszczak, D.K. Lau, L.P. McIntosh, B.J. Graves, Ras signaling requires dynamic properties of Ets1 for phosphorylation-enhanced binding to coactivator CBP, Proc. Natl. Acad. Sci. U. S. A. 107 (2010) 10026–10031.
[39] H. Gao, C. Peng, B. Liang, M. Shahbaz, S. Liu, B. Wang, Q. Sun, Z. Niu, W. Niu, E. Liu, J. Wang, P. Lin, J. Wang, J. Niu, beta6 integrin induces the expression of metalloproteinase-3 and metalloproteinase-9 in colon cancer cells via ERK-ETS1 pathway, Cancer Lett. 354 (2014) 427–437.
[40] D. Hanahan, L.M. Coussens, Accessories to the crime: functions of cells recruited to the tumor microenvironment, Cancer Cell 21 (2012) 309–322.
[41] H.A. Kenny, C.Y. Chiang, E.A. White, E.M. Schryver, M. Habis, I.L. Romero, A. Ladanyi, C.V. Penicka, J. George, K. Matlin, A. Montag, K. Wroblewski, S.D. Yamada, A.P. Mazar, D. Bowtell, E. Lengyel, Mesothelial cells promote early ovarian cancer metastasis through fibronectin secretion, J. Clin. Invest. 124 (2014) 4614–4628.
[42] L. Bruney, Y. Liu, A. Grisoli, M.J. Ravosa, M.S. Stack, Integrin-linked kinase activity modulates the pro-metastatic behavior of ovarian cancer cells, Oncotarget 7 (2016) 21968–21981.
[43] A.K. Mitra, M. Zillhardt, Y. Hua, P. Tiwari, A.E. Murmann, M.E. Peter, E. Lengyel, MicroRNAs reprogram normal fibroblasts into cancer-associated fibroblasts in ovarian cancer, Cancer Discov. 2 (2012) 1100–1108.
[44] Y.H. Wu, T.H. Chang, Y.F. Huang, H.D. Huang, C.Y. Chou, COL11A1 promotes tumor progression and predicts poor clinical outcome in ovarian cancer, Oncogene 33 (2014) 3432–3440.
[45] V.M. Golubovskaya, Targeting FAK in human cancer: from finding to first clinical trials, Front. Biosci. (Landmark Ed. 19 (2014) 687–706.
[46] W. Li, H. Wang, J. Zhang, L. Zhai, W. Chen, C. Zhao, miR-199a-5p regulates beta1 integrin through Ets-1 to suppress invasion in breast cancer, Cancer Sci. 107 (2016) 916–923.

[47] V.P. Dia, E. Gonzalez de Mejia, Lunasin potentiates the effect of oxaliplatin preventing outgrowth of colon cancer metastasis, binds to alpha5beta1 integrin and suppresses FAK/ERK/NF-kappaB signaling, Cancer Lett. 313 (2011) 167–180.

[48] C. Leng, Z.G. Zhang, W.X. Chen, H.P. Luo, J. Song, W. Dong, X.R. Zhu, X.P. Chen, H.F. Liang, B.X. Zhang, An integrin beta4-EGFR unit promotes hepatocellular carcinoma lung metastases by enhancing anchorage independence through activation of FAK-AKT pathway, Cancer Lett. 376 (2016) 188–196.

[49] Y. Kang, W. Hu, C. Ivan, H.J. Dalton, T. Miyake, C.V. Pecot, B. Zand, T. Liu, J. Huang, N.B. Jennings, R. Rupaimoole, M. Taylor, S. Pradeep, S.Y. Wu, C. Lu, Y. Wen, J. Huang, J. Liu, A.K. Sood, Role of focal adhesion kinase in regulating YB-1-mediated paclitaxel resistance in ovarian cancer, J. Natl. Cancer Inst. 105 (2013) 1485–1495.

[50] B. Davidson, V. Givant-Horwitz, P. Lazarovici, B. Risberg, J.M. Nesland, C.G. Trope, E. Schaefer, R. Reich, Matrix metalloproteinases (MMP), EMMPRIN (extracellular matrix metalloproteinase inducer) and mitogen-activated protein kinases (MAPK): co-expression in metastatic serous ovarian carcinoma, Clin. Exp. metastasis 20 (2003) 621–631.

[51] Y. Tanaka, H. Kobayashi, M. Suzuki, Y. Hirashima, N. Kanayama, T. Terao, Genetic downregulation of pregnancy-associated plasma protein-A (PAPP-A) by bikunin reduces IGF-I-dependent Akt and ERK1/2 activation and subsequently reduces ovarian cancer cell growth, invasion and metastasis, International journal of cancer, J. Int. du cancer 109 (2004) 336–347.

[52] Y. Tanaka, H. Kobayashi, M. Suzuki, N. Kanayama, T. Terao, Transforming growth factor-beta1-dependent urokinase up-regulation and promotion of invasion are involved in Src-MAPK-dependent signaling in human ovarian cancer cells, J. Biol. Chem. 279 (2004) 8567–8576.

[53] L. Cao, M. Shao, J. Schilder, T. Guise, K.S. Mohammad, D. Matei, Tissue transglutaminase links TGF-beta, epithelial to mesenchymal transition and a stem cell phenotype in ovarian cancer, Oncogene 31 (2012) 2521–2534.

[54] D. Jia, Z. Liu, N. Deng, T.Z. Tan, R.Y. Huang, B. Taylor-Harding, D.J. Cheon, K. Lawrenson, W.R. Wiedemeyer, A.E. Walts, B.Y. Karlan, S. Orsulic, A COL11A1-correlated pan-cancer gene signature of activated fibroblasts for the prioritization of therapeutic targets, Cancer Lett. 382 (2016) 203–214.